Chinese Journal of Polymer Science Vol. 27, No. 3, (2009), 343–350

Chinese Journal of Polymer Science

MODIFICATION OF POLYAMIDE 6 WITH POLYAMINOAMIDE-*g*-POLY(ETHYLENE GLYCOL) *VIA* HYDROLYTIC POLYMERIZATION*

Yao-chi Liu[a, b], Wei Xu[a], Yuan-qin Xiong[a], Fan Zhang[a] and Wei-jian Xu[a**]

[a] *Institute of Polymer Science & Engineering, Hunan University, Changsha 410082, China*

[b] *College of Urban Construction, Nanhua University, Hengyang 421001, China*

Abstract To enhance the impact strength of polyamide 6, hydrolytic polymerization modification by the polyaminoamide-*g*-poly(ethylene glycol) (PAAEG) derivatives with poly(ethylene glycol) (PEG) molecular weight of 400–10000 was studied. Amide groups of polyaminoamide segments were postulated to form hydrogen bonding with polyamide 6, and hydroxy groups of PAAEG units were expected to react with carboxylic acid groups of polyamide 6 forming copolymers during the polymerization. The improved compatibility in amorphous regions of blends has been confirmed by differential scanning calorimetry (DSC) and scanning electron microscopy (SEM) of fracture surfaces. The effects of PAAEG on the water absorption and notch sensitivity of blends were investigated, using water uptake measurement and mechanical testings, respectively. For comparison, pure polyamide 6 and the blend of PEG/polyamide 6 were also investigated. The addition of PAAEG retarded the crystallization of polyamide 6, but did not make remarkable influences on its crystalline structure. As a consequence of the strong interactions between the dispersed phases and polyamide 6 matrices, PAAEG was a more suitable additive for improving the notched impact strength of polyamide 6 than PEG.

Keywords: Polyamide 6; Polyaminoamide-*g*-poly(ethylene glycol); Blends; Impact strength; Compatibility.

INTRODUCTION

Polymer blends have been extensively studied because of their simplicity, and many new products have been manufactured to achieve improved properties generally not available in any single polymeric material[1–3]. Polyamide 6 (PA6) is a kind of widely used engineering plastics because of its chemical stability and good fatigue[4–7], but its usage is limited by notch sensitivity. Generally, the low temperature impact strength is improved by random incorporation of rubber particles into the nylon 6 matrices. Polyether is the commonly used rubber phase with low glass transition temperature and small domain size[8]. Polymer blends of PA6 and polyether are immiscible because of the positive enthalpy change and the small increase of entropy on mixing. Therefore, the stabilization and enhancement of adhesion between the two phases is very important.

PA6 can be prepared by hydrolytic or anionic polymerization of ε-caprolactam (CL)[9]. A large number of efforts were made to incorporate poly(ethylene glycol) (PEG) into PA6 by anionic polymerization. The block or graft copolymers formed during anionic polymerization act as compatibilizers, which reduces the size of dispersed phase and stabilizes the dispersed phase[10–14]. For hydrolytic polymerization, Fakirov *et al*. investigated multiblock poly(ether-ester-amide)s (PEEA) based on carboxyl-terminated PA6 oligomers and PEG by a two-step polycondensation reaction[15, 16]. Deschamps *et al*. investigated PEEA copolymers based on PEG, 1,4-butanediol and a diester-diamide monomer[17, 18]. These chemical routes however didn't avoid the phase separation between polyamide and PEG because of low esterification capacities resulting in low yields of copolymer. As regards the poor miscibility of polymer pairs, hydrogen bonding, dipolar interactions, phenyl

* This work was financially supported by the National Natural Science Foundation of China (No. 20707008) and China Petroleum & Chemical Corporation.

** Corresponding author: Wei-jian Xu (徐伟箭), E-mail: polymer_group@163.com

Received January 2, 2008; Revised February 23, 2008; Accepted February 29, 2008

group coupling or ionic interactions may also contribute to a negative heat of mixing, making homogeneous polymer blends thermodynamically stable[19].

In this paper, polymer blends of polyaminoamide-*g*-poly(ethylene glycol) (PAAEG) and PA6 were investigated. Instead of using a block or graft copolymer as compatibilizer, we employed PAAEG as the blend component partner directly. Amide groups of polyaminoamide segment and PA6 were postulated to form hydrogen bonding, and hydroxy groups of PAAEG were expected to react with carboxylic acid groups of PA6. Thus, the dispersed PEG phase could easily extend to the PA6 matrix. For comparison, pure PA6 and the blend of PEG2000 (Average molecular weight of PEG is 2000) and PA6 were also investigated.

EXPERIMENTAL

Materials

Epichlorohydrin (ECH) was purified by distillation. CL (China Petroleum & Chemical Corporation), adipic acid (AA) (Sinopharm Chemical Reagent Co., Ltd), diethylene triamine (DETA), hydroxylbenzylthioether (HBTE) and poly(ethylene glycol) [PEG, average molecular weight (M_n): 400, 1000, 2000, 6000 and 10000] were used without further purification.

Synthesis of PAAEG Derivatives

PAAEG derivatives were synthesized by reacting amino terminated polyaminoamide (PAA) with PEG-ECH adduct (Fig. 1). PAA was prepared according to Ref. [20, 21] and PEG-ECH according to Ref. [22, 23]. In a typical experiment, PAA-ethanol solution (containing 0.1 mol DETA) was dropped to a flask with the PEG-ECH adduct (containing PEG400, 0.1 mol). Then, KOH (5.6 g, 0.1 mol) was added, and flask was held at 55°C for 5 h. The solution was purified by filtration and reduced in volume with a rotary evaporator. The product was stored in a vacuum desiccator at 65°C for at least 2 days.

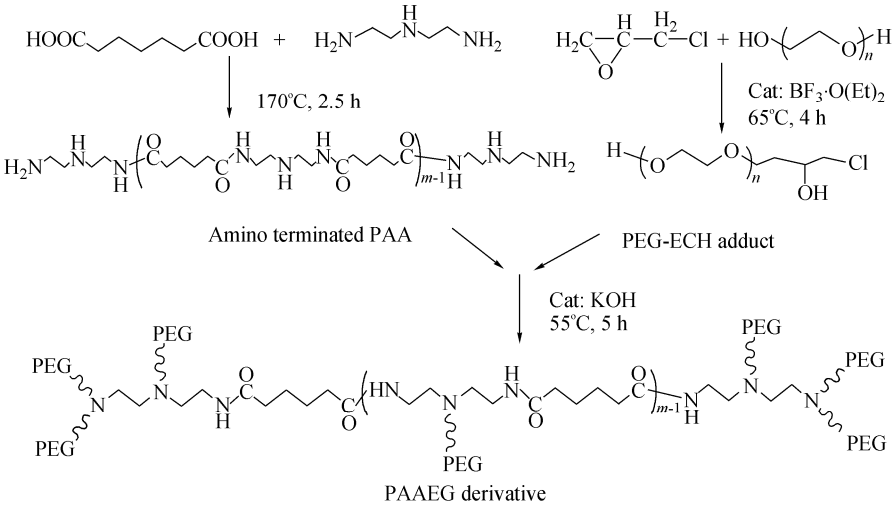

Fig. 1 Synthesis of PAAEG derivatives

Hydrolytic Polymerization

Polymer blends were obtained by hydrolytic polymerization of CL in the presence of PAAEG, initiated by deionized water (DI, 3 wt%). Heat supply was provided by an electric heater and controlled by a stainless rheostat. A stream of dry nitrogen was used to drive off oxygen and vapor in the autoclave before and at the end of polymerization, respectively. For example, in the case of the blend of 3/97 PAAEG400/PA6, PAAEG400 (24.0 g, the molecular weight of PEG is 400), CL (776 g), HBTE (2.4 g) and DI (24 mL) were introduced into a GSH-2 2-L polymerization autoclave at room temperature. The autoclave was heated at a rate of 5 K min^{-1}, held at (275 ± 5)°C and 0.8 MPa for a polymerization time of 3 h, and cooled to 240°C in 1 h. The product was

turned into threads and rapidly cooled to room temperature with water. PA6 threads were turned into fine shavings. The low molecular weight compounds were extracted three times by DI for 8 h.

Characterization

Fourier-transform infrared (FTIR) analysis was performed on a Nicolet Nexus 670 FTIR spectrometer between 4000 cm^{-1} and 400 cm^{-1} in the form of KBr pellets (32 scans, resolution 1 cm^{-1}).

Differential scanning calorimetry (DSC) was performed on Perkin Elmer DSC-7 with sample weight 7–10 mg under nitrogen atmosphere. Each sample, encapsulated in aluminum pans, was heated from 20°C to 300°C at a rate of 10 K min^{-1} before quenching to 50°C at 100 K min^{-1}. Then, the sample was reheated to 300°C at a rate of 10 K min^{-1} at second heating. Crystalline melting temperature (T_m) was obtained as the maximum of melting endotherm. Percentage crystallinity (χ_{DSC}) was calculated *via* the ratio between measured and equilibrium heat of fusion ($\Delta H_f/\Delta H_f^o$). The equilibrium heat of fusion (ΔH_f^o) is 230 J/g for 100% crystalline PA6[24].

X-ray diffraction (XRD) was performed on Rigaku D/Max2500 diffractometer (Ni-filtered, Cu/Kα radiation of wavelength 0.154 nm) in the reflection mode over the range of diffraction angles (2θ) from 5° to 45° at ambient temperature. The voltage and tube current were 40 kV and 200 mA, respectively. Percentage crystallinity by XRD (χ_{XRD}) was calculated by a standard procedure[25].

The morphology of copolymers was observed by scanning electron microscopy (SEM) with a Hitachi S4700 microscope. The cryogenically fractured surfaces of samples were sputter coated with gold to prevent charging in the electron beam.

The samples for water absorption and notched Izod impact were made with an HD-1100 injection machine at a crosshead speed of 50 mm/min. Notched impact tests were conducted according to GB/T1043–1993 after conditioning the samples at 20°C and 65% relative humidity for 24 h. The data were averaged from five repeated measurements. Water absorption measurements were conducted with sheet samples (50 mm × 20 mm × 3.2 mm, length × width × thickness). The dried and weighed samples were emerged in water at ambient temperature for 48 h. Samples were removed, patted dry with a lint free cloth and weighed. The water absorption is expressed as increase in weight percent.

RESULTS AND DISCUSSION

Chemical Bonding between PA6 and PAAEG

Hydrolytic polymerization modification of PA6 studied in this work was performed by PAAEG derivatives with PEG of molecular weight 400–10000. The PAAEG derivatives were synthesized by reacting PAA with PEG-ECH adduct (Fig. 1). PAA, PAAEG400, 6/94 PAAEG400/PA6 and pure PA6 were characterized by FTIR. The majority of the PAA absorption bands (Fig. 2a) are those corresponding to the N—H, C=O, C—H and C—N.

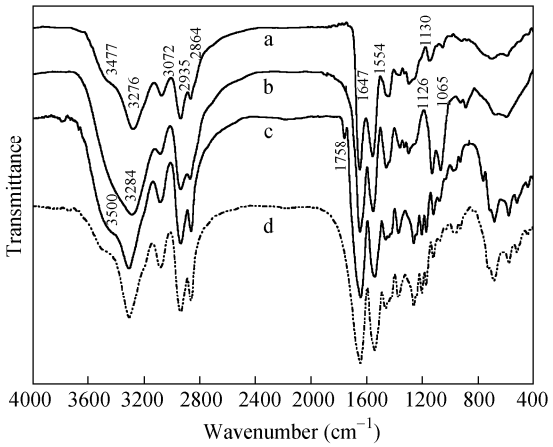

Fig. 2 FTIR spectra of (a) PAA, (b) PAAEG400, (c) 6/94 PAAEG400/PA6 and (d) pure PA6

The N—H and C=O stretching bands are strong, characteristic of the amide function, and appear at 3276 (having a shoulder at 3477 and a weak absorption at 3072) and 1647 cm^{-1}. The N—H deformation can be seen at 1554 cm^{-1}. The C—H stretching consisted of two main absorptions at 2935 and 2864 cm^{-1}. The band that has been most widely reported for secondary amine is the C—N vibration near 1130 cm^{-1}. Figure 2(b) shows the FTIR spectrum of PAAEG400. Compared with PAA, its absorption bands are those corresponding to the O—H and C—O—C moieties. The O—H absorption appears at 3284 and 1065 cm^{-1}, and the C—O—C antisymmetric vibration at 1126 cm^{-1}. The C—N vibration of secondary amine near 1130 cm^{-1} is nearly disappeared. The above results confirm the formation of PAAEG.

Figure 2(c) shows the FTIR spectrum of 6/94 PAAEG400/PA6. In the hydrolytic polymerization system, hydroxy groups of PAAEG can react with carboxylic acid groups of nylon 6 to form graft copolymers, which is characterized by the appearance of a peak at 1758 cm^{-1} corresponding to the ester group. This kind of grafting effect improved the compatibility between PAAEG and nylon 6 (as confirmed in DSC analysis section). But it is worth mentioning that the esterification capacity is relatively low. Compared with pure PA6 (Fig. 2d), 6/94 PAAEG400/PA6 has a strong adsorption shoulder at 3500 cm^{-1}, the characteristic O—H stretching of hydroxy groups. Based on the above results, we would rather call the PAAEG/PA6 system a blend than a graft copolymer.

Influence of PAAEG on Crystallinity of PA6

An accurate investigation of both T_m and χ_{DSC} values was presented by DSC analysis for the blends and pure PA6 (Table 1 and Fig. 3). Both T_m and χ_{DSC} values of PAAEG/PA6 decrease with the increase in PAAEG concentration from 3% to 6% and the decrease in PEG length from 10000 to 400. This decreasing trend is due to the diluent effect of PAAEG additives on the crystallizable portions of PA6 segments, *i.e.*, the compatibility and uniformity between PAAEG and nylon 6 segments, which comes from the interactions of hydrogen bonding and reactive compatibilization. Polyaminoamide segments of PAAEG can form hydrogen bonding with PA6, and the hydroxy groups of PAAEG can react with the carboxylic acid groups of PA6 during polymerization. The fine dispersion of soft segments in the main polymer hinders the regular alignment of PA6 chains and has a strong effect on the nascent structure of PA6. For the blends with the same composition, when PEG lengths decrease from 10000 to 400, the proportions of polyaminoamide and hydroxy group increase, resulting in improved compatibilities. The increase in PAAEG content may also induce evident dilution. Thus, we may infer that PAAEG phase can easily extend to the PA6 matrix for the blend of 6/94 PAAEG400/PA6, so that the packing of PA6 is relatively influenced, and the blend is characterized by low T_m and χ_{DSC} values.

Table 1. Influence of the PAAEG type and concentration on some parameters characterizing blends

Mass composition	T_m[a] (°C)	ΔH_f[b] ($J \cdot g^{-1}$)	χ_{DSC}[c] (%)	χ_{XRD}[d] (%)	α_1[e] ($2\theta°$)	γ[f] ($2\theta°$)	α_2[g] ($2\theta°$)
PAAEG400/PA6 = 3/97	218.9	54.6	23.7	22.8	20.0	–	23.9
PAAEG1000/PA6 = 3/97	219.5	60.6	26.3	25.1	20.0	–	23.9
PAAEG2000/PA6 = 3/97	220.5	63.9	27.8	26.6	20.1	–	23.8
PAAEG6000/PA6 = 3/97	221.1	64.7	28.1	27.0	20.0	–	23.9
PAAEG10000/PA6 = 3/97	221.4	68.3	29.7	28.6	20.1	–	23.8
PAAEG400/PA6 = 6/94	216.8	48.5	21.1	20.9	20.1	–	23.9
PAAEG1000/PA6 = 6/94	219.6	50.1	21.8	20.9	20.0	–	23.9
PAAEG2000/PA6 = 6/94	219.0	52.4	22.8	22.4	20.0	–	23.9
PAAEG6000/PA6 = 6/94	220.2	55.6	24.2	23.0	20.1	21.4	23.8
PAAEG10000/PA6 = 6/94	220.5	61.7	26.8	25.9	20.1	21.4	23.7
PEG2000/PA6 = 6/94	221.3	64.2	27.9	26.2	20.0	–	23.7
Pure PA6	222.4	76.8	33.4	29.7	20.1	21.4	23.9

[a]Melting temperature at second heating; [b]Heat of fusion at second heating; [c]Degree of crystallinity calculated from DSC analysis at second heating; [d]Degree of crystallinity calculated from XRD analysis; [e]Reflection of the crystalline plane (200); [f]Reflection of the crystalline plane (001); [g]Reflection of the crystalline plane (002) + (202)

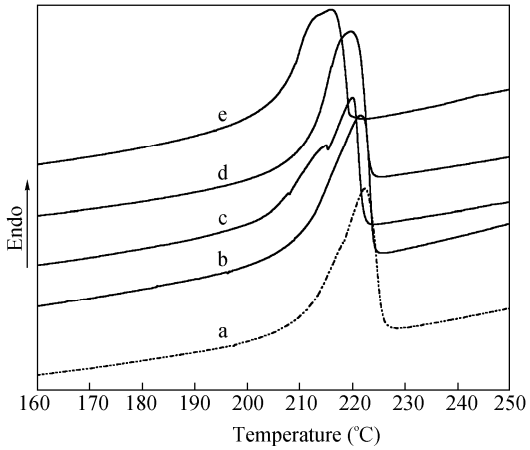

Fig. 3 DSC traces of (a) pure PA6, (b) 6/94 PEG2000/PA6, (c) 6/94 PAAEG6000/PA6, (d) 6/94 PAAEG2000/PA6 and (e) 6/94 PAAEG400/PA6

In the PEG2000/PA6 system, addition of PEG resulted in a slight decrease in the T_m and χ_{DSC} values of PA6 component. This appears to be due to the partial miscibility of PA6 and PEG. Compared with the blend of 6/94 PAAEG2000/PA6, 6/94 PEG2000/PA6 owns higher T_m and χ_{DSC} values. Contributions determining crystalline melting temperature and percentage crystallinity include constitution and molecular structural characteristic. For 6/94 PEG2000/PA6 blend, hydrogen bonding between the dispersed phase and matrix is nonexistent. It is relatively difficult to introduce PEG segments into PA6 matrices, and PEG segments can easily aggregate and produce a coarsening dispersed phase because of poor compatibility (see also Fig. 5c). The relatively higher decrease in the T_m and χ_{DSC} values of PAAEG2000/PA6 however suggests that the interaction between the dispersed phase and the matrix exists sufficiently, resulting in further retardation of crystallization.

For a more detailed comparison with χ_{DSC} values, χ_{XRD} values of pure PA6 and blends were evaluated by the XRD technique (Table 1). The results obtained by XRD have a rather good agreement with those obtained by DSC, although all XRD data are shifted to lower values. The good correspondence between the two sets of data supports the general conclusion drawn above.

Another point worth mentioning is the presence of a shoulder peak of 6/94 PAAEG6000/PA6 blend (Fig. 3c). One possibility is that the PA6 components of blend crystallize in two forms, α and γ [23], as discussed in XRD analysis section and shown in Table 1.

Polymorphism of Modified PA6

Figure 4 shows some XRD intensity profiles of blends and pure PA6 as regards the polymorphism. For comparison, curves of 6/94 PAAEG2000/PA6 (Fig. 4d) and PEG2000/PA6 (Fig. 4c) are put together. The crystalline region of pure PA6 (Fig. 4a) hold the two characteristic peaks of α form at α_1 $2\theta = 20.2°$ and α_2 $2\theta = 23.8°$, corresponding to the reflections of the crystalline planes (200) and (002) + (202), respectively. A careful observation of the intensity profile leads to the identification of a very small percent of γ form at $2\theta =$ 21.4°, corresponding to the reflection of the crystalline plane (001)[21, 23]. In the blends of PAAEG/PA6 and PEG/PA6, the PA6 components almost crystallize in the α form, assumed to be due to the high flexibility of dispersed PEG facilitating crystallization of the polyamide segments in the more perfect α-modification. It is known that PA6 generally shows α form in the case of extended chain conformation or γ form crystalline structure in which the chains are twisted[26]. Thus the addition of PAAEG does not make remarkable influences on the crystalline structure of PA6, notwithstanding the decrease in percentage crystallinity observed by DSC.

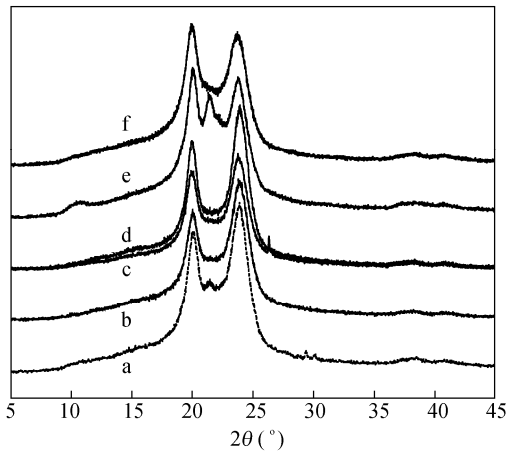

Fig. 4 XRD patterns of (a) pure PA6, (b) 6/94 PAAEG400/PA6, (c) 6/94 PAAEG2000/PA6, (d) 6/94 PEG2000/PA6, (e) 6/94 PAAEG6000/PA6 and (f) annealed 6/94 PAAEG6000/PA6

In Fig. 4(e), a relevant presence of γ form is evident for 6/94 PAAEG6000/PA6, with a sharp peak, which is nonexistent for the blend of 3/97. This may be due to thermal and processing conditions[26]. When the PAAEG concentration is low and the PEG length is short, the strong dipole-dipole interactions between polyamide segments will force the soft segment into the amorphous phase. As the concentration and chain length increase, the mobility of soft segment is relatively confined, especially when the samples are rapidly cooled. In order to further understand this variation in crystallinity, post condensation annealing experiments were carried out above the melting point of PA6 at 230°C under vacuum. Samples were cooled at a rate of 1 K min^{-1}. As expected, the XRD intensity profiles of annealed samples only exhibit α form crystalline (Fig. 4f), *i.e.*, the γ form almost transforms into α form upon annealing.

Morphology of the Blend

SEM analysis is a simple method to clarify phase morphology of PA6 blends[1, 2]. The morphology of 6/94 PAAEG2000/PA6 (Fig. 5b) is similar to that of the pure PA6 (Fig. 5a). The homogeneous distribution suggests that PAAEG was well dispersed in PA6 matrix. The discrete PEG particles observed in the SEM micrograph of fracture surface of 6/94 PEG2000/PA6 (Fig. 5c) however suggests that the interaction between PA6 and PEG is relatively weak, due to the low esterification capacity of hydroxy groups reacting with carboxylic acid groups as aforementioned.

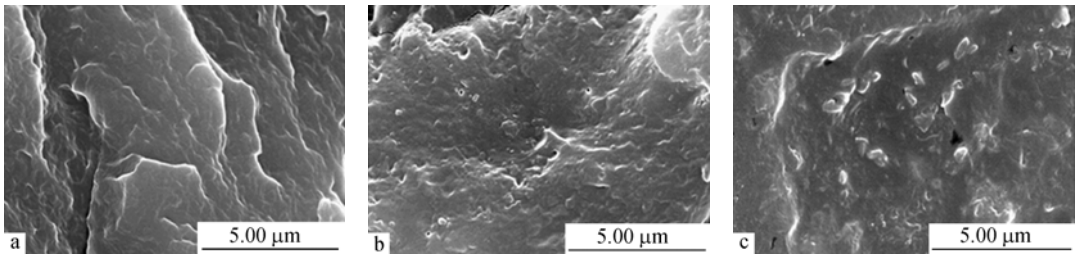

Fig. 5 SEM micrographs of (a) pure PA6, (b) 6/94 PAAEG2000/PA6 and (c) 6/94 PEG2000/PA6

According to the discussion in DSC and SEM sections, we can draw a conclusion that the compatibility of PAAEG/PA6 blend is higher than that of PAAEG/PA6. The possible explanation is the strong interactions consisting of hydrogen boning and reactive compatibilization between PA6 and PAAEG resulting in the enhancement of degree of mixing.

Impact Strength of Modified PA6

It is known that PA6 is sensitive to a notch and has a low energy of crack propagation. In this paper, we focus the mechanical testing of blends on the notched impact strength measurement to investigate the effect of the improved compatibility made by PAAEG on the notched toughness of the final blends. Notched impact strengths of blends and pure PA6 are listed in Table 2. The crystallinity and morphology of blends discussed in the previous sections are closely related to the notched impact strengths of blends. Commonly, an increase in the crystallinity leads to a decrease in the notched impact strength. In the blends of PAAEG/PA6, PAAEG segments serve as inhibitors of crack propagation. As PAAEG content increases and PEG length decreases, the crystallinity of PAAEG/PA6 blend decreases, resulting in the increase of notched impact strength. Compared with pure PA6, more than one-fold higher value at 6/94 PAAEG400/PA6 has been measured.

Table 2. Variations of notched impact strength and percentage water absorption of blends

Mass composition	E_n [a] (kJ·m^{-2})	W_a [b] (%)
PAAEG400/PA6 = 3/97	12.53	9.1
PAAEG1000/PA6 = 3/97	10.14	8.8
PAAEG2000/PA6 = 3/97	9.50	8.6
PAAEG6000/PA6 = 3/97	8.95	8.0
PAAEG10000/PA6 = 3/97	8.86	7.9
PAAEG400/PA6 = 6/94	14.19	11.4
PAAEG1000/PA6 = 6/94	11.00	11.2
PAAEG2000/PA6 = 6/94	10.34	10.6
PAAEG6000/PA6 = 6/94	9.48	10.1
PAAEG10000/PA6 = 6/94	9.72	9.9
PEG2000/PA6 = 6/94	9.86	11.9
Pure PA6	6.48	5.7

[a] Notched impact strength; [b] Percentage water absorption

The notched impact strength of 6/94 PEG2000/PA6 blend is lower than that of 6/94 PAAEG2000/PA6. This result, as expected, is due to the poor miscibility and small interfacial adhesion between PEG and PA6 as mentioned before. PEG segments can easily aggregate and produce a coarsening dispersed phase in the blend, which has been observed on the fracture surface of PEG2000/PA6 blend by SEM.

Water Absorption of Modified PA6

PA6 is semicrystalline and susceptible to water absorption. The absorbed water increases chain mobility and thus will cause dimensional instability with property degradation. In order to study the interaction between water and blends, water absorption measurements were conducted (Table 2). On the whole, the addition of PAAEG or PEG results in an increment of water absorption of blends. As regards the water absorption mechanism of blends, two aspects should be taken into account: the crystallinity and the hydrophilic nature of soft segment. For pure PA6, as the crystallinity increases the amount of water absorption commonly decreases. Water molecules can only diffuse into the amorphous phase and displace 'disordered' amide-amide hydrogen bonds, but they cannot penetrate into the crystal domain and break apart existing amide-amide bonds in this phase. The water absorption of PAAEG/PA6 blends with the same composition also follows the above rule, *e.g*., the blends with a mass composition of 3/97, the decrease in crystallinity from 29.7 of PAAEG10000/PA6 blend to 23.7 of PAAEG400/PA6 blend results in a slight increase in water absorption from 7.9% to 9.1%.

Compared with the crystallinity, the hydrophilic nature of soft segment is a more important factor that affects water absorption. As the content of PAAEG segments increases, an increase in water absorption occurs obviously, *e.g*., the blends of PAAEG400/PA6, the increase in PAAEG content from 3% to 6% increases the water absorption of blends by 2.3% to 11.4%, where the crystallinity decreases slightly from 23.7% to 21.1%. Similarly, because PEG2000 has a stronger affinity for water than PAAEG2000, the blend of 6/94 PEG2000/PA6 possesses higher percentage water absorption than 6/94 PAAEG2000/PA6. As a result, the moisture resistance of PAAEG/PA6 blends is expected to be better than that of PEG/PA6 blends, and the former would display greater dimensional stability.

CONCLUSIONS

PAAEG derivatives with different PEG chain lengths were introduced into PA6 during hydrolytic polymerization of CL. The crystallinity, miscibility, morphology, notched impact strength and water absorption of the PAAEG/PA6 blends were studied. For comparison, pure PA6 and PEG2000/PA6 blends were also investigated.

The decreases in T_m and crystallinity of PA6 suggest that the addition of PAAEG retards the crystallization of polyamide as a result of improved compatibility. The magnitude of the decrease becomes large as increasing PAAEG content and decreasing PEG length. Additional indirect evidence on the improvement of the compatibility can also be obtained from the SEM micrographs of fracture surfaces. The XRD experiments suggest that the addition of PAAEG does not make remarkable influences on the crystalline structure of PA6. Compared with the crystallinity, the hydrophilic nature of PAAEG is a more important factor that affects water absorption. Contrastive experiments suggest that PAAEG is a more suitable additive for improving the notched impact strength of PA6 than PEG. Compared with the blend of PEG/PA6, the blend of PAAEG/PA6 has higher impact strength, better moisture resistance and greater dimensional stability.

ACKNOWLEDGEMENTS The authors thank Prof. Chang-yuan Yu of Beijing University of Chemical Technology for his help in recording SEM micrographs.

REFERENCES

1 Ji, Y., Ma, J. and Liang, B., Mater. Lett., 2005, 59: 1997
2 Harrats, C., Fayt, R. and Jerome, R., Polymer, 2002; 43: 5347
3 Wang, X.C., Yang, G.S. and Zheng, Q., Chinese J. Polym. Sci., 2007, 25(5): 473
4 Freluchea, M., Iliopoulos, I., Flat, J.J., Ruzette, A.V. and Leibler, L., Polymer, 2005, 46: 6554
5 Freluchea, M., Iliopoulos, I., Millequant, M., Flat, J.J. and Leibler, L., Macromolecules, 2006, 39: 6905
6 Pae, Y., J. Appl. Polym. Sci., 2006, 99: 292
7 Pae, Y., J. Appl. Polym. Sci., 2006, 99: 300
8 Pandya, M.V., Subramaniyam, M. and Desai, M.R., Eur. Polym. J., 1997, 33: 789
9 Kim, K.J., Cho, H.W. and Yoon, K.J., Eur. Polym. J., 2003, 39: 1249
10 Yang, H., Morris, J.J. and Lopina, S.T., J. Colloid Interf. Sci., 2004, 273: 148
11 Crespy, D. and Landfester, K., Macromolecules, 2005, 38: 6882
12 Chen, F. and Gu, L., Synth. Fib. Ind.(in Chinese), 1994, 17(2): 15
13 Kim, K.J., Hong, K.S. and Tripathy, A.R., J. Appl. Polym. Sci., 1999, 73: 1285
14 Zuniga, I.A. and Yanez, I.G., Polym. Bull., 2004, 53(1): 25
15 Fakirov, S., Goranov, K., Bosvelieva, E. and Chesne, A.D., Makromol. Chem., 1992, 193: 2391
16 Apostolov, A.A., Bosvelieva, E., Chesne, A.D., Goranov, K. and Fakirov, S., Makromol. Chem., 1993, 194: 2267
17 Deschamps, A.A., Grijpma, D.W. and Feijen, J., J. Biomater. Sci. Polym. Ed., 2002, 13: 1337
18 Deschamps, A.A., Apeldoorn A.A., Bruijn J.D., Grijpma, D.W. and Feijen, J., Biomaterials, 2003, 24: 2643
19 Carone, R., Felisberti, M.I. and Nunes, S.P., J. Mater. Sci., 1998, 33: 3729
20 Liu, W., Ni, Y. and Xiao, H., J. Colloid Interf. Sci., 2004, 275: 584
21 Tu, S., Hu, M. and He, P., Chinese J. Colloid Polym.(in Chinese), 2004, 22(2): 23
22 Li, H.M., Jin, H. and Zhu, H.J., Fine Chem. Interm.(in Chinese), 2005, 35(3): 45
23 Song, W., Huang, W. and Jin, Y., Chem. Ind. Times(in Chinese), 2004, 18(8): 33
24 Udipi, K., Dave, R.S., Kruse, R.L. and Stebbins, L.R., Polymer, 1997, 38(4): 927
25 Mateva, R., Petrov, P., Rousseva, S., Dimitrov, R. and Zolova, G., Eur. Polym. J., 2000, 36: 813
26 Yu, Y.C. and Jo, W.H., J. Appl. Polym. Sci., 1995, 56: 895